Dissection of the Physiological Interconversion of 5α-DHT and 3α-Diol by Rat 3α-HSD via Transient Kinetics Shows That the Chemical Step Is Rate-Determining: Effect of Mutating Cofactor and Substrate-Binding Pocket Residues on Catalysis†

Vladi V. Heredia‡ and Trevor M. Penning*,§

Departments of Biochemistry & Biophysics and Pharmacology, University of Pennsylvania School of Medicine, Philadelphia, Pennsylvania 19104

Received May 20, 2004; Revised Manuscript Received July 21, 2004

ABSTRACT: 3α-Hydroxysteroid dehydrogenases (3α-HSDs) catalyze the interconversion between 5α-dihydrotestosterone (5α-DHT), the most potent androgen, and 3α-androstanediol (3α-diol), a weak androgen metabolite. To identify the rate-determining step in this physiologically important reaction, rat liver 3α-HSD (AKR1C9) was used as the protein model for the human homologues in fluorescence stopped-flow transient kinetic and kinetic isotope effect studies. Using single and multiple turnover experiments to monitor the NADPH-dependent reduction of 5α-DHT, it was found that k_{lim} and k_{max} values were identical to k_{cat}, indicating that chemistry is rate-limiting overall. Kinetic isotope effect measurements, which gave $^{D}k_{cat} = 2.4$ and $^{D_2O}k_{cat} = 3.0$ at pL 6.0, suggest that the slow chemical transformation is significantly rate-limiting. When the $NADP^+$-dependent oxidation of 3α-diol was monitored, single and multiple turnover experiments showed a k_{lim} and burst kinetics consistent with product release as being rate-limiting overall. When NAD^+ was substituted for $NADP^+$, burst phase kinetics was eliminated, and k_{max} was identical to k_{cat}. Thus with the physiologically relevant substrates 5α-DHT plus NADPH and 3α-diol plus NAD^+, the slowest event is chemistry. R276 forms a salt-linkage with the phosphate of 2′-AMP, and when it is mutated, tight binding of NAD(P)H is no longer observed [Ratnam, K., et al. (1999) *Biochemistry 38*, 7856−7864]. The R276M mutant also eliminated the burst phase kinetics observed for the $NADP^+$-dependent oxidation of 3α-diol. The data with the R276M mutant confirms that the release of the NADPH product is the slow event; and in its absence, chemistry becomes rate-limiting. W227 is a critical hydrophobic residue at the steroid binding site, and when it is mutated to alanine, k_{cat}/K_m for oxidation is significantly depressed. Burst phase kinetics for the $NADP^+$-dependent turnover of 3α-diol by W227A was also abolished. In the W227A mutant, the slow release of NADPH is no longer observed since the chemical transformation is now even slower. Thus, residues in the cofactor and steroid-binding site can alter the rate-determining step in the $NADP^+$-dependent oxidation of 3α-diol to make chemistry rate-limiting overall.

Sex steroid target tissues convert steroid precursors into potent hormones, a process known as intracrine formation (*1*, *2*). Because the hormones produced locally may contribute to diseases of the prostate and breast, the enzymes involved in the local formation of steroid hormones are attractive drug targets. For example, in the prostate, testosterone is converted by 5α-reductase type 2 to 5α-dihydrotestosterone (5α-DHT[1]) (*3*), the most potent androgen with a K_d of 10^{-11} M for its receptor (*4*, *5*). In diseases such as benign prostatic hyperplasia (BPH) or prostatic adenocarcinoma (PCA), overproduction of 5α-DHT is suspect in disease progression (*6*, *7*); and its formation can be blocked by the 5α-reductase type 2 inhibitor finasteride (*8*, *9*). 3α-Hydroxysteroid dehydrogenases (3α-HSDs) eliminate 5α-DHT by forming 3α-androstanediol (3α-diol), a weak androgen with an affinity of 10^{-6} M for the androgen receptor (Scheme 1) (*4*, *5*). Thus 3α-HSDs play a functional role in the removal of the androgen signal.

HSDs belong to two protein superfamilies: short-chain dehydrogenases/reductases (SDR) (*10*) and aldo-keto reductases (AKR[2]) (*11*, *12*). Mammalian 3α-HSDs belong to the AKR superfamily, which are mostly monomeric, soluble, NAD(P)(H)-dependent oxidoreductases (*4*). We have recently identified human type 3 3α-HSD (AKR1C2) as the AKR

† This work was supported by NIH Grant DK47015 to T.M.P.

* To whom correspondence should be addressed: Department of Pharmacology, University of Pennsylvania School of Medicine, 130C John Morgan Building, 3620 Hamilton Walk, Philadelphia, PA 19104-6084. Tel: (215) 898-9445. Fax: (215) 573-2236. E-mail: penning@pharm.med.upenn.edu.

‡ Department of Biochemistry & Biophysics.

§ Department of Pharmacology.

[1] Abbreviations: HSD, hydroxysteroid dehydrogenase; 3α-HSD, 3α-hydroxysteroid dehydrogenase (EC 1.1.1.213, A-face specific and designated as AKR1C9); 5α-DHT, 5α-dihydrotestosterone or 17β-hydroxy-5α-androstan-3-one; 3α-diol, 3α-androstanediol or 5α-androstane-3α-17β-diol; AKR, aldo-keto reductase; SDR, short-chain dehydrogenase/reductase; KIE, kinetic isotope effect.

[2] The nomenclature for the aldo-keto reductase superfamily was recommended by the 8th International Symposium on Enzymology & Molecular Biology of Carbonyl Metabolism, Deadwood, SD, June 29−July 3, 1996.

10.1021/bi0489762 CCC: $27.50
Published on Web 09/02/2004

Scheme 1: Reaction Scheme for 5α-DHT Reduction and 3α-Diol Oxidation by AKR1C9 with Various Cofactors

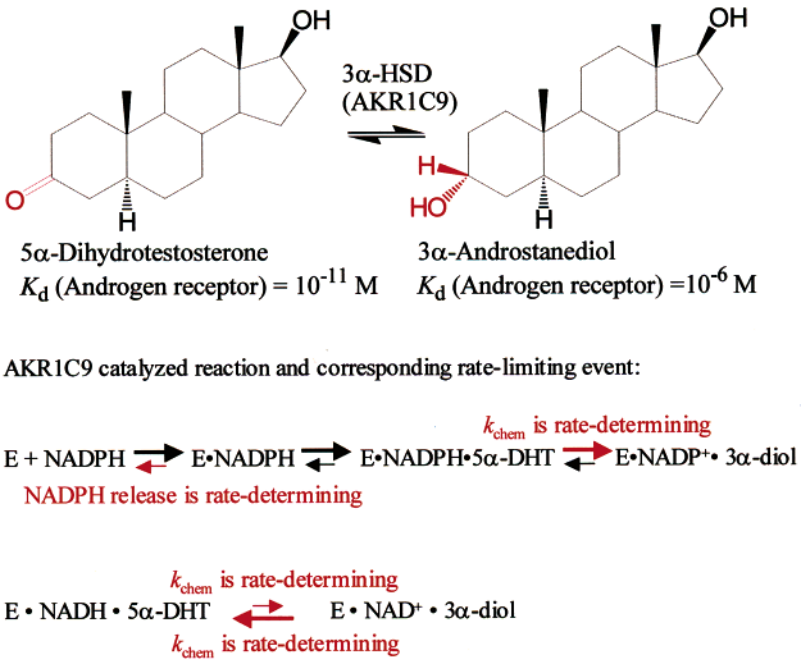

responsible for the elimination of 5α-DHT in peripheral tissues (*13*, *14*). However, the rate-determining step in the transformation of the physiologically relevant substrate pair 5α-DHT to 3α-diol and vice versa by any AKR is unknown. AKR1C2 shares greater than 67% amino acid identity with rat liver 3α-HSD (AKR1C9), the most extensively studied steroid transforming AKR. Because of the high sequence identity that exists, structure−function studies on the rat enzyme are likely to be applicable to the human homologue.

AKR1C9 displays an ordered bi-bi kinetic mechanism in which binding of the nicotinamide cofactor is an obligatory requirement before steroid hormone can bind (*15*). In the ternary complex, the 4-*pro-R* hydride is transferred from NADP(H) to the acceptor carbonyl on the steroid substrate which is protonated by Y55 that acts as a general acid/base (*15*, *16*). Crystal structures reveal that the nicotinamide cofactor lies perpendicular to the steroid ligand. Comparisons of the apoenzyme structure, the binary complex of E·$NADP^+$ and the ternary complex of E·$NADP^+$·testosterone show that significant conformational changes occur during the sequential binding of its ligands (*17*−*19*). AKR1C9 is highly regioselective and stereospecific in that, unlike its human homologues, only 3-ketosteroids are recognized and reduced (*14*, *20*). It is this strict requirement for 3-ketosteroids and high catalytic efficiencies that makes ARK1C9 highly amenable for mechanistic studies.

We have utilized stopped-flow kinetics to determine which steps are rate-limiting in the reduction of 5α-DHT and which steps are rate-limiting in the oxidation of its cognate inactive metabolite, 3α-diol by AKR1C9. Concurrently, primary and solvent kinetic isotope effect (KIE) measurements were performed. We find that while the rate of 3α-diol oxidation is limited by the rate of release of NADPH, for the physiological substrate pairs 5α-DHT with NADPH and 3α-diol with NAD^+, the rate-limiting step is the chemical event. We also find that discrete point mutations in the cofactor and steroid binding site can alter the rate-determining step for the $NADP^+$-dependent oxidation of 3α-diol.

EXPERIMENTAL PROCEDURES

Materials. Expression and purification of AKR1C9 and its mutants R276M and W227A have been described previously (*21*, *22*). Final specific activities of the enzymes utilized in this study are 1.6, 1.7, and 0.006 μmol androsterone oxidized/min/mg, respectively. The cofactors NAD(H) and NADP(H) were obtained from Roche Diagnostics. The steroids 5α-DHT and 3α-diol were purchased from Steraloids. Deuterium oxide (D_2O), deuterated ethanol, sodium deuteroxide, and deuterium chloride were purchased from Cambridge Isotope Laboratories. $NADP^+$-specific alcohol dehydrogenase from *Leuconostoc mesenteroides* was purchased from Research Plus, Inc. All other reagents were purchased from Sigma and are ACS grade or better.

Synthesis and Purification of 4-pro-R-[^{2}H]NADPH. 4-*pro-R*-[^{2}H]-NADPH was synthesized by the method of Viola et al. (*23*) and Jeong et al. (*24*) with minor modifications. The reaction was performed in 25 mM Tris buffer, pH 8.6 at 25 °C with deuterated ethanol and $NADP^+$ as cofactor, using $NADP^+$-specific *L. mesenteroides* alcohol dehydrogenase. The reaction was followed to completion by monitoring the change in absorbance at 340 nm. The products were separated from the enzyme using an Amicon centrifugal filter device. The unreacted ethanol and the product acetaldehyde were removed by rotary evaporation. [^{2}H]-NADPH was purified by subjecting the remaining mixture to anion exchange chromatography on a Whatman DE-52 column, equilibrated in 10 mM Tris buffer, pH 8.0 and eluted using a 0−2.75% NaCl linear gradient. Fractions with A_{260}/A_{340} ratios of 2.3 or less were pooled and lyophilized. An aliquot of the pooled [^{2}H]-NADPH was analyzed by ^{1}H NMR. The degree of deuteration was evaluated on the basis of the chemical shifts of protons in the nicotinamide ring, as described previously (*23*, *25*, *26*). The disappearance of the N4 proton resonance at δ 8.9 in $NADP^+$ on stereospecific deuteration to (4*R*)-[^{2}H]-NADPH was used to assess that reduction was complete. The degree of deuteration was monitored by the

absence of a double doublet for the N4 proton resonances at δ 2.9 and its replacement by a broad singlet for the single 4-*pro*-S methine proton at δ 2.9. On the basis of this change in splitting patterns, the deuterated cofactor was determined to be >99% pure (*24*, *27*, *28*). The concentration was calculated using A_{340}, with $\epsilon_{340} = 6270\ M^{-1}\ cm^{-1}$.

Determination of Dissociation Constants for Cofactors. K_d values for the binding of the cofactors to AKR1C9 and its mutants were determined by measuring protein fluorescence on a Hitachi F-4500 fluorescence spectrophotometer following the incremental addition of NAD(H) (20−500 μM) and NADP(H) (40 nM to 100 μM). Each sample contained 0.20 μM protein in 10 mM potassium phosphate, pH 7.0 buffer containing 1 mM EDTA at 25 °C. Care was taken to ensure that the volume of cofactor added was not more than 2% of the total volume. Samples were excited at 290 nm with fluorescence emission scanned from 300 to 500 nm with slit widths set at 5 nm. A modified Scatchard analysis was used to calculate K_d values (*22*, *29*). Briefly, the fractional saturation (α) by the ligand of the total ligand binding sites was equated to $\Delta F/\Delta F_{max}$, where ΔF is the change in fluorescence at a given ligand concentration and ΔF_{max} is the change in fluorescence at fully saturating ligand concentration. K_d values were determined using eq 1, whereby α is related to L_O, the total ligand concentration, and E_O, the total active-site concentration.

$$L_O/\alpha = K_d/(1 - \alpha) + E_O \quad (1)$$

The slope of a plot of 1/(1-α) versus L_O/α yields K_d, and the *y*-intercept yields the concentration of available binding sites.

Steady State Kinetics. Initial rates were measured on a Hitachi F-4500 fluorescence spectrophotometer. Excitation and emission wavelengths were set at 340 and 450 nm, respectively. The rate of change in fluorescence emission of the cofactor at 450 nm was monitored to determine initial velocities. Assays were performed in 1-mL systems containing 10 mM potassium phosphate, pH 7.0 buffer containing 4% acetonitrile at 25 °C. All reactions were initiated by the addition of enzyme and were corrected for nonenzymatic rates. Standard curves with known reduced cofactor concentrations were constructed on a daily basis. Calculation of k_{cat} and K_m values used GRAFIT 5.0 (Erithacus Software) by fitting untransformed data with a hyperbolic function, as originally described by Wilkinson (*30*), to yield estimates of kinetic constants and their associated standard errors.

Steady state kinetic parameters for the NADPH-dependent reduction of 5α-DHT catalyzed by AKR1C9 and W227A were determined at 50 μM NADPH while the steroid concentration was varied between 0.1 and 30 μM 5α-DHT. For the R276M mutant, rates for the NADPH-dependent reduction of 5α-DHT were determined at 100 μM NADPH. Steady state rates for the NADH-dependent reduction of 5α-DHT by AKR1C9 were determined at 500 μM NADH. The steady state kinetic parameters for the oxidation of 3α-diol with $NAD(P)^+$ catalyzed by AKR1C9, R276M, and W227A enzymes were determined at 2.3 mM cofactor concentration while the steroid concentration was varied between 1 and 75 μM 3α-diol. In each instance, the cofactor concentration was saturating with respect to the enzyme form.

Primary Kinetic Isotope Effects. To determine the primary KIE, the [^{2}H]-NADPH-dependent conversion of 5α-DHT by wild type, R276M, and W227A enzymes was monitored as described above. Because 3α-HSD undergoes an acid/base-catalyzed reaction with Y55 acting as the general acid/base, the pH profile indicates that 5α-DHT reduction is optimal at pH 6.0 (*16*). Therefore, primary KIEs were determined at pH 6.0 in order to obtain values in the pH-independent range of the pH−k_{cat} profile and at pH 7.0 in order to obtain values at physiological pH. Primary KIEs were calculated by fitting initial velocities to eq 2,

$$v = k_{cat}[E][A]/\{K_m\,(1 + FE_{k_{cat}/K_m}) + [A](1 + FE_{k_{cat}})\} \quad (2)$$

where F is the fraction of deuterium label in the substrate, E_{k_{cat}/K_m} and $E_{k_{cat}}$ are the isotope effects minus 1 on k_{cat} and k_{cat}/K_m, respectively, E is the enzyme concentration, and A is the concentration of varied substrate. Primary KIEs are reported using the nomenclature of Northrop (*31*) whereby $^Dk_{cat}$ is the ratio of k_{cat} determined in the presence of NADPH relative to k_{cat} determined in the presence of [^{2}H]-NADPH. Similarly, $^Dk_{cat}/K_m$ is the ratio of k_{cat}/K_m determined in the presence of NADPH relative to the k_{cat}/K_m determined in the presence of [^{2}H]-NADPH.

Solvent Kinetic Isotope Effects. Buffers prepared in D_2O were adjusted to the desired pL value with either sodium deuteroxide or deuterium chloride using a pH meter. Appropriate corrections were made to the meter reading according to the formula pD = (meter reading) + 0.4 (*32*). Enzymes were exchanged using Centricon ultrafiltration into the appropriate D_2O buffer so that all protonated amino acid residues are deuterated. This process was performed 5 times to ensure complete equilibration of the deuterated solvent with enzyme.

Solvent KIEs for the NADPH-dependent reduction of 5α-DHT catalyzed by the wild type and mutant enzymes ($^{D_2O}k_{cat}$ and $^{D_2O}k_{cat}/K_m$) were determined by performing assays in H_2O and D_2O at 10 mM potassium phosphate buffer containing 4% acetonitrile at 25 °C and were carried out as described above. Initial rates were determined under conditions in which the catalytic rates were pL independent (pL 6.0) and under physiological conditions (pL 7.0). Solvent KIEs were determined by fitting initial velocities to eq 2. Solvent KIEs are reported using the nomenclature of Northrop (*31*) whereby $^{D_2O}k_{cat}$ is the ratio of k_{cat} determined in H_2O to k_{cat} determined in D_2O. Similarly, $^{D_2O}k_{cat}/K_m$ is the ratio of k_{cat}/K_m determined in H_2O relative to the k_{cat}/K_m determined in D_2O.

Transient State Kinetics. Transient state kinetic experiments were performed using an Applied Photophysics SX.18MV-R stopped flow reaction analyzer at 25 °C. The instrument was set in fluorescence mode with excitation at 340 nm and emission monitored using a 450 nm band-pass filter. Reactions were performed in 10 mM potassium phosphate buffer at pH 7.0 containing 4% acetonitrile. Standard curves with known NAD(P)H concentrations were constructed on a daily basis. The change in fluorescence signal was monitored as a function of time for the cofactor dependent reduction of 5α-DHT and oxidation of 3α-diol. For single turnover experiments, enzyme was incubated with limiting NAD(P)(H) in one syringe and varying concentrations of steroid substrates were introduced into the stopped-

flow apparatus by means of a second syringe, and reactions were initiated by rapid mixing of the two solutions. For multiple turnover experiments, enzyme was incubated with excess NAD(P)(H) in one syringe and varying concentration of steroid substrates were introduced by means of a separate syringe, and reactions were initiated by rapid mixing of the two solutions. The kinetic transients obtained were analyzed and rate constants determined using the Applied Photophysics SX18.MV-R software v. 4.46, based on robust nonlinear regression (Marquardt) algorithm. For single turnover experiments, rate constants (k_{obs}) were determined from single exponential fits to averages of 5−10 traces per steroid concentration. For multiple turnover experiments, averages of 5−10 traces per steroid concentration were fit to either eq 3, for traces which exhibit a burst phase and linear phase kinetics, or eq 4, for traces which exhibit a linear phase only:

$$y = Ae^{(-k_{burst}t)} + k_{ss}t + C \quad (3)$$

where y = signal, A = amplitude of burst, t = time, and C = intercept, and

$$y = k_{ss}t + C \quad (4)$$

where y = signal, t = time, and C = intercept.

Equation 3 determines the rate of the burst (k_{burst}) and the rate of the linear steady state portion (k_{ss}) while eq 4 determines k_{ss} only. Plots of k_{burst} versus steroid concentration were fit to the hyperbolic equation (eq 5) and show $k_{max(burst)}$, the maximum rate of the burst phase.

$$k_{ss} \text{ or } k_{burst} = \frac{k_{max}[\text{substrate}]}{K_d + [\text{substrate}]} \quad (5)$$

Plots of k_{ss} versus steroid concentration were also fitted to eq 4 to determine $k_{max(ss)}$ and K_m.

RESULTS

Single and Multiple Turnover Experiments for 5α-DHT Reduction. Single turnover and multiple turnover experiments were performed to monitor the NADPH-dependent reduction of 5α-DHT. Using wild type enzyme, single turnover experiments were performed with limiting NADPH concentrations so that the enzyme could not recycle. Each transient showed single exponential kinetics; and plots of k_{obs} versus steroid concentration gave saturation kinetics with a maximal value denoted as k_{lim} (Figure 1A and Table 1). The k_{lim} for 5α-DHT reduction was 0.44 s^{-1} and was in agreement with the k_{cat} for 5α-DHT reduction, where k_{cat} is the rate constant for the overall reaction in the steady state. K_d values obtained from the hyperbola also gave reasonable values reflective of substrate binding (Supporting Information). Single turnover experiments could not be performed with NADH since AKR1C9 has very low affinity for NADH; consequently it was not technically feasible to saturate sufficient enzyme (1−5 μM) with enough cofactor to generate a signal of sufficient amplitude.

Multiple turnover experiments were performed with excess NADPH to determine whether burst phase kinetics were observed upon the rapid mixing of the E·NADPH binary complex with increasing steroid concentrations (Figure 1C). The turnover of 5α-DHT did not exhibit burst kinetics; only the linear steady state portion of the reaction was detected. Plots of k_{ss} versus steroid concentration fit saturation kinetics; and the k_{max} of the linear steady state rate of 5α-DHT reduction by NADPH (0.34 s^{-1}) was in agreement with the k_{lim} derived under single turnover conditions (0.44 s^{-1}) and the k_{cat} derived under steady state conditions (0.30 s^{-1}). When E·NADH and 5α-DHT were rapidly mixed under multiple turnover conditions, no burst of NADH formation was observed (Figure 1E) and the k_{max} of the linear phase (0.39 s^{-1}) was identical to the k_{cat} value determined in the steady state (0.43 s^{-1}). K_m values obtained from fitting multiple turnover data from both series of experiments to eq 5 gave values identical to those observed in the steady state (Supporting Information). These results suggest that, irrespective of the cofactor utilized, chemistry is rate-limiting in the reduction of 5α-DHT.

Single and Multiple Turnover Experiments for 3α-Diol Oxidation. Single turnover and multiple turnover experiments were performed to monitor the $NADP^+$-dependent oxidation of 3α-diol. Single turnover experiments were performed with limiting $NADP^+$ concentrations so that the enzyme could not recycle. Each treatment showed a single exponential; and plots of k_{obs} versus steroid concentration gave saturation kinetics with a maximal value denoted as k_{lim} (Figure 1B). The k_{lim} for 3α-diol oxidation was 42.4 s^{-1} and was 2 orders of magnitude greater than the k_{cat} observed in the steady state (Table 1).

Multiple turnover experiments were performed with excess $NADP^+$ to determine whether burst phase kinetics was observed for 3α-diol oxidation. Indeed, a burst of product formation (NADPH) was detected whereby the amplitude of the burst coincided with the enzyme concentration present in the reaction (Figure 1D). The k_{burst} fit saturation kinetics over the range of steroid concentration used, and the k_{max} of the burst (50 s^{-1}) coincided with the k_{lim} for the single turnover experiments. The k_{max} for the linear steady state rate in the multiple turnover experiment was significantly less than the k_{max} of the burst and agreed with the k_{cat} for the reaction observed in the steady state.

When these experiments were replicated with NAD^+, different phenomena were observed. Under single turnover conditions, the k_{lim} at saturating steroid concentration was in agreement with k_{cat} observed in the steady state. Furthermore, no burst phase kinetics was observed under multiple turnover conditions for 3α-diol oxidation (Figure 1F).

The K_d value for 3α-diol derived from single turnover conditions using $NADP^+$ was 30 μM, while the K_m values derived under multiple turnover conditions using $NADP^+$ and NAD^+ were 6.3 μM and 20 μM, respectively. The former value is indicative of the affinity of 3α-diol for the E·$NADP^+$ binary complex; and the latter two values are consistent with the K_m values obtained under steady state conditions (Supporting Information). Collectively, these results suggest that product release is rate-limiting when $NADP^+$ is utilized, but that chemistry is rate-limiting when NAD^+ is substituted.

Primary and Solvent Kinetic Isotope Effects for 5α-DHT Reduction. Because AKR1C9 exhibited a k_{lim} value identical to k_{cat} under single turnover conditions and no burst kinetics under multiple turnover conditions, we wanted to validate that chemistry was indeed rate-limiting for the reduction of 5α-DHT. Primary KIEs were determined in the transformation of 5α-DHT using saturating deuterated cofactor ([^{2}H]-

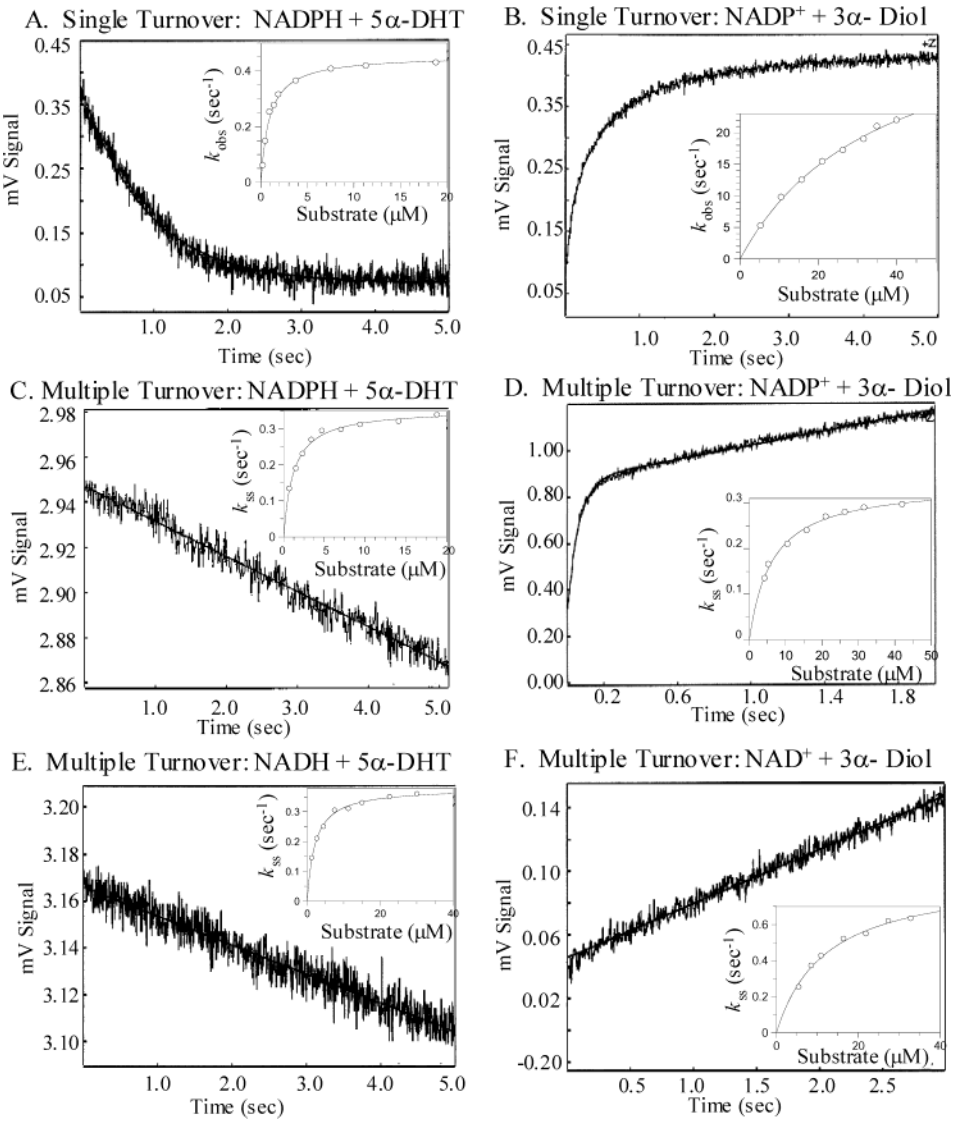

FIGURE 1: Representative transient kinetic traces for the transformation of 5α-DHT and 3α-diol by wild type enzyme. A and B are single turnover stopped flow progress curves, and C−F are multiple turnover stopped flow progress curves. Graphs depict the average from 5−10 traces of progress curves in fluorescence mode with excitation at 340 nm and emission monitored using a 450 nm band-pass filter. Reactions were performed in 10 mM phosphate buffer, pH 7.0 at 25 °C and 4% acetonitrile. The transient trace in A was the result of mixing 0.5 μM 3α-HSD with 0.5 μM NADPH in the first syringe and 11.3 μM 5α-DHT in the second syringe. The transient trace in B was the result of mixing 0.5 μM 3α-HSD with 0.5 μM $NADP^+$ in the first syringe and 10.5 μM 3α-diol in the second syringe. First-order rate constants (k_{obs}) were determined by fitting data to a single exponential equation over a range of steroid concentrations. The transient trace in C was the result of mixing 0.5 μM 3α-HSD with 30 μM NADPH in the first syringe and 18.5 μM 5α-DHT in the second syringe. The transient trace in D was the result of mixing 0.5 μM 3α-HSD with 30 μM $NADP^+$ in the first syringe and 26.3 μM 3α-diol in the second syringe. The transient trace in E was the result of mixing 2 μM 3α-HSD with 500 μM NADH in syringe 1 and 15.7 μM 5α-DHT in syringe 2. The transient trace in F was the result of mixing 2 μM 3α-HSD with 1.25 mM NAD^+ in syringe 1 and 10.5 μM 3α-diol in syringe 2. For C, E, and F, rate constants for the steady state (k_{ss}) were obtained by fitting data to the linear regression equation over a range of steroid concentrations. For D, first-order rate constants for the burst phase (k_{burst}) and the steady state rate constant (k_{ss}) were obtained by fitting data to the equation for a single exponential plus steady state. The transient curve in D emphasizes the pre steady state burst in 3α-diol oxidation using $NADP^+$ cofactor. Insets to A and B are plots of k_{obs} versus [steroid substrate] with hyperbolic curve fits to the data, which show saturation kinetics. Insets to C−F are plots of k_{ss} versus [steroid substrate] which show saturation kinetics for the linear steady state phase of the reactions.

NADPH) at pH 7.0 and pH 6.0. For the wild type protein, the $^{D}k_{cat}$ and $^{D}k_{cat}/K_m$ determined at physiological pH were 2.36 and 2.03, respectively (Table 2). The primary KIE at pH 6.0 increased slightly to give values of 2.43 and 2.31 for $^{D}k_{cat}$ and $^{D}k_{cat}/K_m$, respectively. Solvent KIE measurements indicated a significant solvent effect with $^{D_2O}k_{cat}$ of 3.02 and $^{D_2O}k_{cat}/K_m$ of 3.33 when reactions were performed at pL 6.0, the pL-independent portion of k_{cat} (where changes in pL do not alter the reaction rate).

Effect of R276M and W227A Mutants on Microscopic Rate Constants for Substrate Turnover. Previous studies on the R276M mutant showed that removal of the guanidinium side chain disrupted the salt linkage that exists between R276 and the 2′-phosphate of NADP(H) (*21*). This change eliminated the tight binding of NADP(H) for AKR1C9, and as a result, the mutant had similar K_d values for NADP(H) and NAD(H) (Supporting Information). In examining the effect of this mutant on the reduction of 5α-DHT by

Table 1: Comparison of k_{cat} with the Microscopic Rate Constants Detected in the Transient State for the Transformation of 5α-DHT and 3α-Diol Catalyzed by AKR1C9 and Its Mutants

enzyme	substrates	k_{cat} in steady state (s^{-1})	k_{lim} of single turnover (s^{-1})	k_{max} of burst in multiple turnover (s^{-1})	k_{max} of steady state in multiple turnover (s^{-1})
AKR1C9	NADPH + 5α-DHT	0.30 ± 0.0021	0.44 ± 0.0084	none	0.34 ± 0.0079
	$NADP^+$ + 3α-diol	0.37 ± .014	42.4 ± 4.1	50.2 ± 2.1	0.34 ± 0.0024
	NADH + 5α-DHT	0.43 ± 0.040	*a*	none	0.39 ± 0.021
	NAD^+ + 3α-diol	0.85 ± .078	*a*	none	0.87 ± 0.054
R276M	NADPH + 5α-DHT	0.40 ± 0.011	*a*	none	0.48 ± 0.0072
	$NADP^+$ + 3α-diol	0.80 ± 0.027	*a*	none	0.90 ± 0.031
W227A	NADPH + 5α-DHT	0.037 ± 0.0012	0.033 ± .0022	none	0.043 ± 0.0027
	$NADP^+$ + 3α-diol	$6.3 \times 10^{-4} \pm 8.3 \times 10^{-6}$	$7.2 \times 10^{-4} \pm 1.7 \times 10^{-5}$	none	$6.9 \times 10^{-4} \pm 1.6 \times 10^{-5}$

[a] Since the wild type and the R276M mutant have a very low affinity for NAD(H) and NADP(H), respectively (Supporting Information), single turnover determinations were not feasible.

Table 2: Kinetic Isotope Effects in the NADPH-Dependent Reduction of 5α-DHT by AKR1C9 and Its Mutants

enzyme	$^{D}k_{cat}$[a,b]	$^{D}k_{cat}/K_m$[a,b]	$^{D_2O}k_{cat}$[b]	$^{D_2O}k_{cat}/K_m$[b]
	A. Values Derived from Measurements at pL 7.0			
AKR1C9	2.36 ± 0.01 (6)	2.03 ± 0.09 (6)	1.73 ± 0.013 (5)	1.71 ± 0.003 (5)
R276M	2.29 ± 0.17 (3)	2.15 ± 0.17 (3)	1.89 ± 0.04 (4)	2.01 ± 0.11 (4)
W227A	2.33 ± 0.10 (5)	2.47 ± 0.12 (5)	2.52 ± 0.11 (5)	2.80 ± 0.13 (5)
	B. Values Derived from Measurements at pL 6.0			
AKR1C9	2.43 ± 0.03 (6)	2.31 ± 0.08 (6)	3.02 ± 0.09 (5)	3.33 ± 0.09 (5)
R276M	2.35 ± 0.19 (3)	2.39 ± 0.23 (3)	2.80 ± 0.10 (4)	2.75 ± 0.12 (4)
W227A	2.66 ± 0.13 (5)	2.15 ± 0.21 (5)	5.11 ± 0.51 (3)	5.14 ± 0.12 (3)

[a] All primary KIEs were measured with saturating cofactor with 5α-DHT as the varied substrate. [b] The values in parentheses denote number of individual determinations.

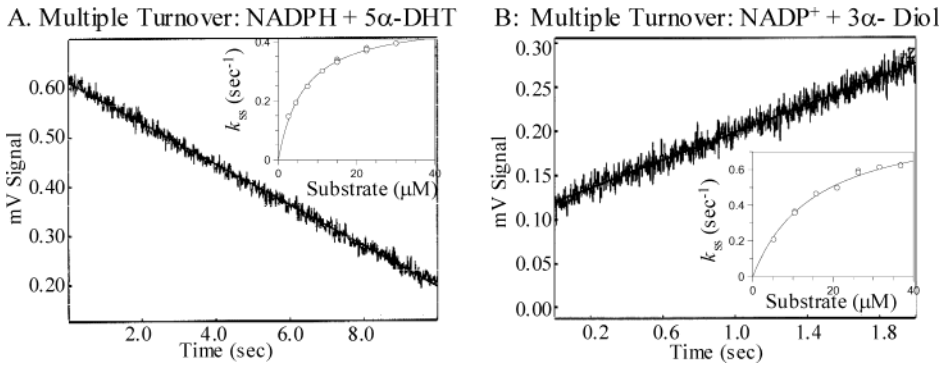

FIGURE 2: Representative transient kinetic traces for the transformation of 5α-DHT and 3α-diol by R276M under multiple turnover conditions. Curves depict the average from 5−10 traces of multiple turnover stopped-flow progress curves set in fluorescence mode with excitation at 340 nm and emission monitored using a 450 nm band-pass filter. Reactions were performed in 10 mM phosphate buffer, pH 7.0 at 25 °C and 4% acetonitrile. The transient trace in A was the result of mixing 2 μM R276M with 100 μM NADPH in the first syringe and 11.3 μM 5α-DHT in the second syringe. The transient trace in B was the result of mixing 2 μM R276M with 250 μM $NADP^+$ in the first syringe and 10.9 μM 3α-diol in the second syringe. Rate constants for the steady state (k_{ss}) were obtained by fitting data to the linear regression equation over a range of steroid concentrations. Insets are plots of k_{ss} versus [steroid substrate] which show saturation kinetics for the linear steady state phase of the reaction.

NADPH, we predicted that there would be no change in its transient kinetic profile. However, in the oxidation of 3α-diol by $NADP^+$, we anticipated that the burst phase kinetics seen with the wild type enzyme would be eliminated if the release of the NADPH product were rate-determining.

For the R276M mutant, only multiple turnover conditions were achievable because of the high K_d of this mutant for the NADP(H) cofactors. In monitoring the reduction of 5α-DHT by NADPH catalyzed by the R276M mutant, the k_{ss} at saturation was identical to k_{cat} in the steady state (Figure 2). In monitoring the oxidation of 3α-diol by $NADP^+$, the burst phase was eliminated, and the k_{ss} at saturation was equal to k_{cat} in the steady state.

Previous studies on the W227A mutant showed that the removal of the indole ring and its substitution by the methyl group of alanine led to steroid "wobble" at the active site, which not only resulted in large decreases in the k_{cat} values for the turnover of hydroxysteroid substrates but also changed the rate-limiting step for androsterone oxidation (*22*). Here we used this same mutant to examine the role of W227 in the 3α-HSD-catalyzed interconversion of its physiological substrates. Because this mutant does not affect the K_d for cofactors (Supporting Information), both single and multiple turnover experiments could be performed (Figure 3). For the NADPH-dependent reduction of 5α-DHT, the k_{lim} for single turnover was equal to k_{cat} in the steady state, and no burst phase kinetics was observed. For the $NADP^+$-dependent oxidation of 3α-diol, single turnover experiments exhibited saturation kinetics with a k_{lim} equal to k_{cat}. Under multiple

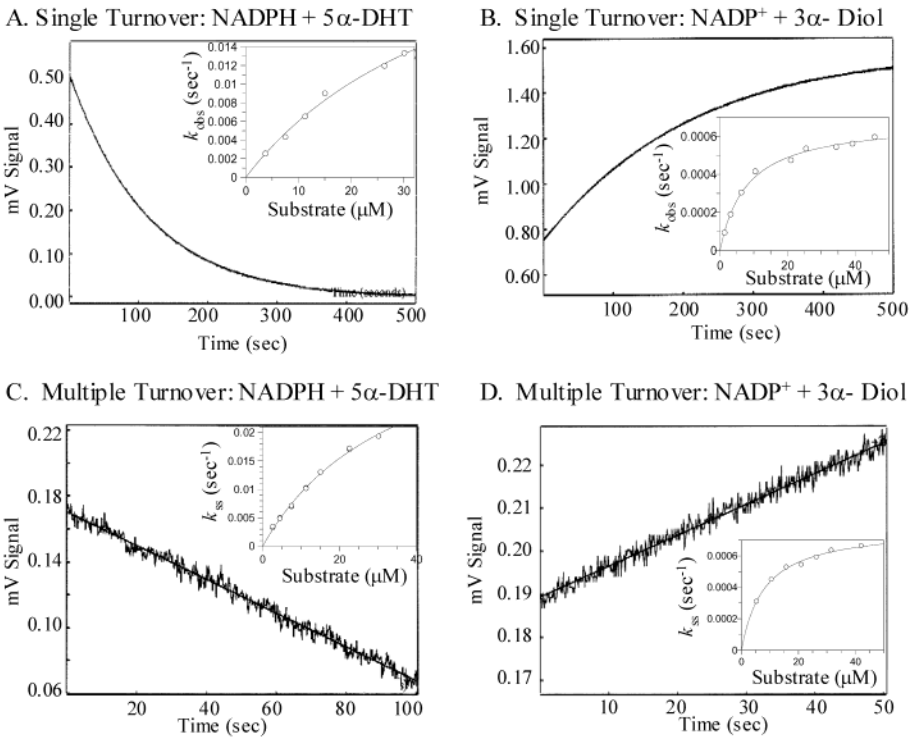

FIGURE 3: Representative transient kinetic traces for the transformation of 5α-DHT and 3α-diol by the W227A mutant. A and B are single turnover stopped flow progress curves, and C and D are multiple turnover stopped flow progress curves. Graphs depict the average from 5−10 traces of progress curves in fluorescence mode with excitation at 340 nm and emission monitored using a 450 nm band-pass filter. Reactions were performed in 10 mM phosphate buffer pH 7.0 at 25 °C and 4% acetonitrile. The transient trace in A was the result of mixing 0.5 μM W227A with 0.5 μM NADPH in the first syringe and 16.4 μM 5α-DHT in the second syringe. The transient trace in B was the result of mixing 1.0 μM W227A with 1.0 μM NADP$^+$ in the first syringe and 30 μM 3α-diol in the second syringe. First-order rate constants (k_{obs}) were determined by fitting data to a single exponential equation over a range of steroid concentrations. The transient trace in C was the result of mixing 0.5 μM W227A with 30 μM NADPH in the first syringe and 7.5 μM 5α-DHT in the second syringe. The transient trace in D was the result of mixing 1.0 μM W227A with 30 μM NADP$^+$ in the first syringe and 10.5 μM 3α-diol in the second syringe. Rate constants for the steady state (k_{ss}) were obtained by fitting data to the linear regression equation over a range of steroid concentrations. Insets to A and B are plots of k_{obs} versus [steroid substrate] with hyperbolic curve fits to the data, which show saturation kinetics. Insets to C and D are plots of k_{ss} versus [steroid substrate] which show saturation kinetics for the linear steady state phase of the reaction.

turnover conditions, burst phase kinetics were again eliminated, and k_{ss} was equal to k_{cat}.

Primary and Solvent Isotope Effects for 5α-DHT Reduction Catalyzed by the R276M and W227A Mutants. Because no burst of product was observed in the multiple turnover of 5α-DHT with NADPH by the R276M and W227A mutants, we expected a primary isotope effect when [^{2}H]-NADPH was utilized and/or a solvent isotope effect when reactions were carried out in D_2O. Results indicate that the mutations retained the KIEs observed in the wild type protein (Table 2). For the R276M mutant, the $^Dk_{cat}$ was 2.4 and the $^{D_2O}k_{cat}$ was 2.8 at pL 6.0. For the W227A mutant, the $^Dk_{cat}$ was 2.7 and the $^{D_2O}k_{cat}$ was 5.1 at pL 6.0.

DISCUSSION

The Rate-Limiting Step in Rat 3α-HSD. AKR1C enzymes catalyze the interconversion between the potent androgen 5α-DHT with the inactive metabolite 3α-diol in androgen target tissues (*13*, *20*). The microscopic events that define this physiologically relevant transformation were examined using transient state kinetics and kinetic isotope effect measurements. Using rat liver 3α-HSD as the protein model, we find that substrates, cofactors, and discrete residues in the binding pocket all play significant roles in rate determination. A summary of the major findings is illustrated in Scheme 1.

The conditions for single turnover experiments were designed so that the enzyme could only go through a single pass of catalysis and not recycle. Because no lag phase was observed when steroid was mixed with the enzyme−cofactor complex, steroid binding is not a slow event. Thus the events monitored are based solely on the rates of steroid transformation and product release. Transient traces obtained under single turnover conditions indicate that chemistry is rate-determining in the NADPH-dependent reduction of 5α-DHT, which is supported by a k_{lim} value that equals the k_{cat} value observed in the steady state. Furthermore, no burst of NADP$^+$ formation was observed under multiple turnover conditions, and k_{max} of the linear phase was again equal to k_{cat} obtained under steady state conditions.

Isotope effects were measured at physiological pH and at the pH independent portion of the pH−k_{cat} profile for 5α-DHT reduction. The presence of KIEs indicates that the chemical step is a significant contributor to the rate-limiting step. While primary KIE values suggest that hydride transfer plays a role in the rate-determining step, the solvent KIE is more pronounced than the primary KIE at pH 6.0. Unlike primary isotope effects which monitor changes in the catalytic rate associated with only one isotopic substitution, solvent KIEs are multifactorial in nature because they monitor the changes associated with complete replacement

of exchangeable hydrogens with deuterons on the enzyme and substrate (*33*). Solvent effects may be indicative of other factors that alter the rate by affecting substrate binding, multiple steps in the chemical sequence, and/or the conformation of the enzyme (*33*). Hence, the asymmetry between the primary and solvent KIEs in the NADPH-dependent reduction of 5α-DHT may be due to a combination of these factors.

For the $NADP^+$-dependent oxidation of 3α-diol, the k_{lim} values determined from single turnover experiments exceeded the k_{cat} value by over 100-fold, which suggests that the chemical transformation is not rate-limiting. Under multiple turnover conditions, a burst of product (NADPH) formation was observed, which confirms that a subsequent step after chemistry, specifically, product release, is rate-limiting overall.

Pre steady state kinetics of cofactor binding to and release from 3α-HSD using mutagenesis and fluorescence stopped flow techniques showed that the enzyme undergoes a two-step binding mechanism concomitant with a slow conformational change upon NADP(H) binding in which the microscopic rate constants were larger than k_{cat}, the rate of the overall reaction (*21*). A more recent investigation on cofactor binding to rat 3α-HSD was performed in which evidence for a three-step binding model was presented (*34*). Kinetic transients of NADP(H) binding were best fit to a biexponential composed of a fast phase and a slow phase. Unlike the initial study, the microscopic rate of NADPH release in the slow phase approaches the k_{cat} value. Thus in the oxidation direction using $NADP^+$ as cofactor, NADPH release may become partially rate-limiting. Our studies support this conclusion.

Catalysis Using NADP(H) versus NAD(H) Cofactors. The microscopic rate constants that define the rate-limiting step were found to be cofactor-dependent. Using 5α-DHT and NADH as the substrate pair, the k_{max} of the linear phase under multiple turnover conditions was equal to the k_{cat} in the steady state, and no burst phase kinetics was observed. Using 3α-diol and NAD^+ as the substrate pair, the k_{max} of the linear phase under multiple turnover conditions was again equal to the k_{cat} in the steady state, and no burst phase was detected. Thus chemistry is rate-limiting for the NADH-dependent reduction of 5α-DHT and the NAD^+-dependent oxidation of 3α-diol. Interestingly, the rate of 3α-diol oxidation is apparently higher when NAD^+ is used instead of $NADP^+$ (k_{cat} with $NAD^+ = 51\ min^{-1}$ vs k_{cat} with $NADP^+ = 22\ min^{-1}$). One interpretation is that the increase in k_{cat} may arise since the slow release of NADPH, which is rate-determining, no longer occurs. Because the major cellular reducing cofactor is NADPH and the major cellular oxidative cofactor is NAD^+ (*35*, *36*), our studies suggest that, under physiological conditions, the reduction of 5α-DHT by NADPH is dictated by the slow chemical transformation. Similarly, the oxidation of 3α-diol by NAD^+ is also dictated by the slow chemical event.

Role of R276 in Rate Determination. In the 3α-HSD·$NADP^+$ binary complex, the 2′-phosphate of $NADP^+$ forms a salt bridge with R276 (*18*). Previous studies on other AKRs have examined the roles of residues that make contact with the 2′-phosphate group of NADP(H) and indicate that the electrostatic link that forms between the enzyme and the 2′-phosphate is a major reason why most AKRs have a higher affinity for NADP(H) than NAD(H) (*37*−*39*). Formation of this salt bridge is responsible for the isomerization of E·NADP(H) → E*·NADP(H) which is observed as a fluorescence kinetic transient (*21*). We investigated the role of R276 on the catalytic cycle of 3α-HSD with its physiological substrates.

The binding affinity of R276M for NADP(H) is much lower than for wild type enzyme. Furthermore, the binding affinity of R276M for NADP(H) is similar to the binding affinity of wild type enzyme for NAD(H), in that their K_d values are both in the μM range (Supporting Information). This loss in cofactor affinity, however, does not result in large decreases in turnover number. On the contrary, the k_{cat} value for 5α-DHT reduction is retained by the R276M mutant and, interestingly, the k_{cat} value for the $NADP^+$-dependent oxidation of 3α-diol is better for the R276M mutant than the wild type protein. The transient kinetic properties observed for the reduction of 5α-DHT by NADPH and the oxidation of 3α-diol by $NADP^+$ catalyzed by R276M are similar to those observed with AKR1C9 when NAD(H) is substituted. More importantly, the R276M mutant eliminates the burst phase observed in the $NADP^+$-dependent oxidation of 3α-diol by wild type enzyme. This finding confirms that the slow release of product in the oxidation direction is due to NADPH release in AKR1C9. The macroscopic and microscopic events observed are similar between the R276M mutant and the wild type enzyme when $NADP^+$ and NAD^+ are utilized, respectively. Because the rate-determining step associated with NADPH release is abolished in the oxidation direction by this mutation, chemistry has become rate-determining. This also allows for an increase in the overall k_{cat}, albeit a subtle one (a 2-fold change in value), for the $NADP^+$-dependent oxidation of 3α-diol.

In summary, once the R276 anchor for the 2′-phosphate of NADP(H) is removed from the protein, the enzyme treats NADP(H) as it would NAD(H). Residue 276 makes the important distinction between the two cofactors. The ability of AKR1C9 to discriminate between NADP(H) and NAD(H) leads to differential effects in cofactor affinity (NADP(H) ≫ NAD(H)), in mechanism (binding events since a unique fluorescence transient is involved: E·NADP(H) ↔ E*·NADP(H)), and in catalysis (chemistry is rate-limiting for steroid transformation in both directions with NAD(H) but not with NADP(H)).

Role of W227 in Rate Determination. An alignment of putative steroid binding site residues between the rat and human isoforms (AKR1C1−1C4, AKR1C9) shows that while some variability exists, certain residues are highly conserved. Available crystal structures suggest that W227 is a consistently conserved residue in the AKR1C subfamily and interacts with the B and C rings of the steroid by providing a hydrophobic surface in-plane with the steroid (*19*, *40*). In order to understand its function, we examined the role of W227 in the interconversion of the physiologically relevant substrate pair, 5α-DHT and 3α-diol.

In the NADPH-dependent reduction of 5α-DHT catalyzed by the W227A mutant, no burst of product was observed under multiple turnover conditions, and the k_{lim} obtained under single turnover conditions was identical to the k_{cat} obtained in the steady state. The primary and solvent kinetic isotope effects with this mutant were substantial and support

the transient kinetic finding that the chemical step is again rate-determining. Interestingly, during the W227A-catalyzed transformation of 5α-DHT, a large solvent kinetic isotope effect was observed ($^{D_2O}k_{cat} = 5.1$) at pL 6.0. This suggests that the proton donation event becomes even more rate-limiting than before. Large solvent KIEs arise when a rate-determining step involves direct proton transfer in the transition state (*33*). Because of the magnitude of the solvent effect for W227A, the solvent KIE is essentially a primary KIE, whereby proton donation is the largest contributor to the rate-determining step.

The pL dependence on the solvent KIE for W227A is not due to the titration of an active site residue. Y55 is the general acid/base for catalysis (*16*), and mutation of W227 should not lead to a change in the titration curve for this residue. However, W227A does cause a 5- to 30-fold increase in the K_d for steroid, suggesting that binding is impaired (*22*). Impaired binding may either disrupt the proximity between the 3-ketosteroid and Tyr55 (causing steroid wobble) or lead to an insertion of a water molecule between the 3-ketosteroid substrate and Tyr55. The crystal structure of the binary complex provides evidence for an added water molecule at the active site tyrosine. In either instance, a more pronounced solvent KIE may be anticipated.

In the $NADP^+$-dependent oxidation of 3α-diol catalyzed by the W227A mutant, transient kinetics showed that, under single turnover conditions, the k_{lim} obtained at saturation was identical to k_{cat}. Furthermore, no burst of product was observed under multiple turnover conditions. In the oxidation of 3α-diol, the W227A mutation not only resulted in large decreases in steroid turnover but also changed the rate-determining step from NADPH release to chemistry for the formation of 5α-DHT.

An unexpected finding with W227A was the opposing effects on k_{cat} and K_m observed in the reduction and oxidation directions. In the reduction of 5α-DHT, the k_{cat} value only decreased by 9-fold relative to the wild type, but the change in K_m was more substantial (70-fold change). In contrast, during the oxidation of 3α-diol, the k_{cat} value was severely depressed (almost 600-fold decrease) but a negligible change in K_m (less than 2-fold) was observed with this mutant. A previous study in which residues in the testosterone binding pocket of AKR1C9 were systematically mutated to alanine showed that, in the oxidation of 3α-hydroxysteroids, k_{cat} was more adversely affected than either K_m or K_d (*22*). Our findings with the $NADP^+$-dependent oxidation of 3α-diol support this earlier study; however, the opposing effects on 5α-DHT were unexpected.

The differential effects observed with the W227A mutant on the reduction of 5α-DHT and the oxidation of 3α-diol could be explained as follows. Mutating this residue to an alanine may adversely affect the reaction trajectory (*41*, *42*) in the oxidation direction only; thus k_{cat} is depressed and the rate-determining step becomes chemistry. This could result from the structure of the steroid substrate itself. The hybridization state of the reactive center at C3 is sp^3 for oxidation and sp^2 for reduction. Maintenance of the position of the chiral center for the stereospecific oxidation of 3α-diol is likely to be more difficult than the maintenance of the sp^2 group for the reduction of 5α-DHT. Thus, a change in the steroid binding pocket leads to more dramatic changes on k_{cat} for substrates that are oxidized versus substrates that are reduced.

Rate-Determining Step in AKRs. A primary concern in the study of AKR mechanisms is the identification of the rate-determining step. Studies on aldose reductase or AKR1B1, an enzyme closely related to rat 3α-HSD, indicated that the rate-determining step in the reduction of xylose was the slow release of $NADP^+$, as supported by burst kinetics under multiple turnover conditions of xylitol formation (*43*). In the oxidation of xylitol, chemistry was the largest contributor to k_{cat} as no burst of NADPH production was observed under multiple turnover conditions. On the basis of the crystal structure of AKR1B1, the formation of the tight $E^*{\cdot}NADP^+$ complex was thought to be due to the movement of loop B, in which R276 is located (*44*).

This work on the mechanism of steroid transformation, specifically on the physiological substrates 5α-DHT and 3α-diol by AKR1C9, provides new insights into AKR catalysis. Conserved cofactor and steroid binding pocket residues are important for the maintenance of the rate-limiting events in steroid turnover as depicted by the R276M and W227A mutants. The rate-determining step for AKR1C9 is the reverse of aldose reductase when NADP(H) is utilized as the cofactor. The presence of a nucleotide "safety belt" in AKR1B1 and its absence in AKR1C9 may account for this mechanistic difference between the two AKRs. When NAD(H) is utilized by the enzyme, the chemical step is rate-limiting. With the physiological substrate pairs 5α-DHT plus NADPH and 3α-diol plus NAD^+, chemistry appears to be rate-determining in both directions.

ACKNOWLEDGMENT

We gratefully acknowledge the valuable discussions and technical support of Dr. Yi Jin and Dr. William Cooper. We also thank Dr. Sridhar Gophishetty for assistance with the NMR.

SUPPORTING INFORMATION AVAILABLE

K_d values for the cofactors and steady state kinetic constants for cofactors and substrates. K_d and K_m values for fitting transient state kinetic data to eq 5. This material is available free of charge via the Internet at http://pubs.acs.org.

REFERENCES

1. Labrie, F., Luu-The, V., Lin, S.-X., Simard, J., Labrie, C., El-Alfy, M., Pelletier, G., and Belanger, A. (2000) Intracrinology: role of the family of 17β-hydroxysteroid dehydrogenases in human physiology and disease, *J. Mol. Endocrinol. 25*, 1−6.
2. Labrie, F., Luu-The, V., Lin, S.-X., Labrie, C., Simard, J., Breton, R., and Belanger, A. (1997) The key role of 17β-hydroxysteroid dehydrogenases in sex steroid biology, *Steroids 62*, 148−158.
3. Russell, D. W., and Wilson, J. D. (1994) Steroid 5α-reductase: two genes/two enzymes, *Annu. Rev. Biochem. 63*, 25−61.
4. Penning, T. M. (1997) Molecular endocrinology of hydroxysteroid dehydrogenases, *Endocr. Rev. 18*, 281−305.
5. Penning, T. M., Bennett, M. J., Smith-Hoog, S., Schlegel, B. P., Jez, J. M., and Lewis, M. (1997) Structure and function of 3α-hydroxysteroid dehydrogenase, *Steroids 62*, 101−111
6. Davies, P., and Eaton, C. L. (1991) Regulation of prostate growth, *J. Endocrinol. 131*, 5−17.
7. Griffiths, K., and Morton, M. S. (1999) in *Textbook of prostate cancer: pathology, diagnosis and treatment* (Dunitz, M., and Malden, M. A., Eds.) pp 51−74, Blackwell, London.

8. Bull, H. G., Garcia-Calvo, M., Andersson, S., Baginsky, W. E., Chan, H. K., Ellsworth, D. E., Miller, R. R., Stearns, R. A., Bakshi, R. K., Rasmusson, G. H., Tolmna, R. L., Myers, R. W., Kozarich, J. W., and Harris, G. S. (1996) Mechanism-based inhibition of human steroid 5α-reductase by finasteride: enzyme-catalyzed formation of $NADP^+$−dihydrofinasteride, a potent bisubstrate analog inhibitor, *J. Am. Chem. Soc. 118*, 2359−2365.
9. Gormley, G. J. (1996) 5α-Reductase inhibitors in prostate cancer, *Endocr.-Relat. Cancer 3*, 57−63.
10. Jornvall, H., Persson, M., Krook, M., Atrian, S., Gonzalez-Duarte, R., Jeffery, J., and Ghosh, D. (1995) Short-chain dehydrogenases/reductases (SDR), *Biochemistry 34*, 6003−6013.
11. Jez, J. M., Flynn, T. G., and Penning, T. M. (1997) A new nomenclature for the aldo-keto reductase superfamily, *Biochem. Pharmacol. 54*, 639−647.
12. Jez, J. M., Bennett, M. J., Schlegel, B. P., Lewis, M., and Penning, T. M. (1997) Comparative anatomy of the aldo-keto reductase superfamily, *Biochem. J. 326*, 625−636.
13. Rizner, T. L., Lin, H. K., Peehl, D. M., Steckelbroeck, S., Bauman, D. R., and Penning, T. M. (2003) Human type 3 3α-hydroxysteroid dehydrogenase (aldo-keto reductase 1C2) and androgen metabolism in prostate cells, *Endocrinology 144*, 2922−2932.
14. Penning, T. M., Burczynski, M. E., Jez, J. M., Hung, C.-F., Lin, H.-K., Ma, H., Moore, M., Palackal, N., and Ratnam, K. (2000) Human 3α-hydroxysteroid dehydrogenase isoforms (AKR1C1-AKR1C4) of the aldo-keto reductase superfamily: functional plasticity and tissue distribution reveals roles in the inactivation and formation of male and female sex hormones, *Biochem. J. 351*, 67−77.
15. Askonas, L. J., Ricigliano, J. W., and Penning, T. M. (1991) The kinetic mechanism catalysed by homogeneous rat liver 3α-hydroxysteroid dehydrogenase. Evidence for binary and ternary dead-end complexes containing non-steroidal anti-inflammatory drugs, *Biochem. J. 278*, 835−841.
16. Schlegel, B. P., Jez, J. M., and Penning, T. M. (1998) Mutagenesis of 3α-hydroxysteroid dehydrogenase reveals a "push−pull" mechanism for proton transfer in aldo-keto reductases, *Biochemistry 37*, 3538−3548.
17. Hoog, S. S., Pawlowski, J. E., Alzari, P. M., Penning, T. M., and Lewis, M. (1994) Three-dimensional structure of rat liver 3α-hydroxysteroid/dihydrodiol dehydrogenase: a member of the aldo-keto reductase superfamily, *Proc. Natl. Acad. Sci. U.S.A. 91*, 2517−2521.
18. Bennett, M. J., Schlegel, B. P., Jez, J. M., Penning, T. M., and Lewis, M. (1996) Structure of 3α-hydroxysteroid/dihydrodiol dehydrogenase complexed with $NADP^+$, *Biochemistry 35*, 10702−10711.
19. Bennett, M. J., Albert, R. H., Jez, J. M., Ma, H., Penning, T. M., and Lewis, M. (1997) Steroid recognition and regulation of hormone action: crystal structure of testosterone and $NADP^+$ bound to 3α-hydroxysteroid/dihydrodiol dehydrogenase, *Structure 5*, 799−812.
20. Steckelbroeck, S., Jin, Y., Gopishetty, S., Oyesanmi, B., and Penning, T. M. (2004) Human cytosolic 3α-hydroxysteroid dehydrogenases (3α-HSDs) of the aldo-keto reductase (AKR) superfamily display significant 3β-hydroxysteroid dehydrogenase (3β-HSD) activity: Implications for steroid hormone metabolism and activation, *J. Biol. Chem. 279*, 10784−10795.
21. Ratnam, K., Ma, H., and Penning, T. M. (1999) The arginine 276 anchor for NADP(H) dictates fluorescence kinetic transients in 3α-hydroxysteroid dehydrogenase, a representative aldo-keto reductase, *Biochemistry 38*, 7856−7864.
22. Heredia, V. V., Cooper, W. C., Kruger, R. G., Jin, Y., and Penning, T. M. (2004) Alanine scanning mutagenesis of the testosterone binding site of rat 3α-hydroxysteroid dehydrogenase demonstrates contact residues influence the rate-determining step, *Biochemistry 43*, 5832−5841.
23. Viola, R. E., Cook, P. F., and Cleland, W. W. (1979) Stereoselective preparation of deuterated reduced nicotinamide adeninedinucleotides and substrates by enzymatic synthesis, *Anal. Biochem. 96*, 334−340.
24. Jeong, S. S., and Gready, J. E. (1994) A method of preparation and purification of (4R)-deuterated-reduced nicotinamide adenine dinucleotide phosphate, *Anal. Biochem. 221*, 273−277.
25. Stone, S. R., and Morrison, J. F. (1982) Kinetic mechanism of the reaction catalyzed by dihydrofolate reductase from *Escherichia coli*, *Biochemistry 21*, 3757−3765.
26. Beard, W. A., Appleman, J. R., Delcamp, T. J., Freisheim, J. H., and Blakley, R. L. (1989) Hydride transfer by dihydrofolate reductase. Causes and consequences of the wide range of rates exhibited by bacterial and vertebrate enzymes, *J. Biol Chem. 264*, 9391−9399.
27. Oppenheimer, N. J., Arnold, L. J., and Kaplan, N. O. (1978) Stereospecificity of the intramolecular association of reduced pyridine coenzymes, *Biochemistry 17*, 2613−2619.
28. Oppenheimer, N. J. (1987) in *Pyridine nucleotide coenzymes: Part A* (Dolphin, D., Avaramovic, O., and Poulson, R., Eds.), pp 185−203, Wiley, New York.
29. Ehrig, T., Bohren, K. M., Prendergast, F. G., and Gabbay, K. H. (1994) Mechanism of aldose reductase inhibition: binding of $NADP^+$/NADPH and alrestatin-like inhibitors, *Biochemistry 33*, 7157−7165.
30. Wilkinson, G. N. (1961) Statistical estimations in enzyme kinetics, *Biochem. J. 80*, 324−332.
31. Northrop, D. B. (1982) Deuterium and tritium kinetic isotope effects on initial rates. *Methods Enzymol. 87*, 607−625.
32. Schowen, K. B., and Schowen, R. L. (1982) Solvent isotope effects of enzyme systems, *Methods Enzymol. 87*, 551−606.
33. Schowen, R. L. (1977) Solvent isotope effects on enzymatic reactions, in *Isotope effects on enzyme catalyzed reactions* (Cleland, W. W., O'Leary, M. H., and Northrop, D. B., Eds.) pp 64−99, University Park Press, Baltimore, MD.
34. Penning, T. M., Jin, Y., Heredia, V. V., and Lewis, M. (2003) Structure-function relationships in 3α-hydroxysteroid dehydrogenases: a comparison of the rat and human isoforms, *J. Steroid Biochem. Mol. Biol. 85*, 247−255.
35. Krebs, H. A. (1973) Pyridine nucleotides and rate control, *Symp. Soc. Exp. Biol. 27*, 299−318.
36. Reich, J. G., and Selkov, E. E. (1981) *Energy Metabolism of the Cell: A Theoretical Treatise*, Academic Press, New York.
37. Bohren, K. M., Page, J. L, Shankar, R., Henry, S. P., and Gabbay, K. H. (1991) Expression of human aldose and aldehyde reductases. Site-directed mutagenesis of a critical lysine 262, *J. Biol. Chem. 266*, 24031−24037.
38. Kubiseski, T. J., and Flynn, T. G. (1995) Studies on human aldose reductase, *J. Biol. Chem. 270*, 16911−16917.
39. Matsuura, K., Tamada, Y., Sato, K., Iwasa, I., Miwa, G., Deyashiki, Y., and Hara, A. (1997) Involvement of two basic residues (Lys-270 and Arg-276) of human liver 3α-hydroxysteroid dehydrogenase in NADP(H) binding and activation by sulphobromophthalein: site-directed mutagenesis and kinetic analysis, *Biochem. J. 322*, 89−93.
40. Jin, Y., Stayrook, S. E., Albert, R. H., Palackal, N. T., Penning, T. M., and Lewis, M. (2001) Crystal structure of human type III 3α-hydroxysteroid dehydrogenase/bile acid binding protein complexed with $NADP^+$ and ursodeoxycholate, *Biochemistry 40*, 10161−10168.
41. Mesecar, A. D., Stoddard, B. L., and Koshland, D. E., Jr. (1997) Orbital steering in the catalytic power of enzymes: small structural changes with large catalytic consequences, *Science 277*, 202−206.
42. Koshland, D. E., Jr., and Neet, K. E. (1968) The catalytic and regulatory properties of enzymes, *Annu. Rev. Biochem. 37*, 359−410.
43. Grimshaw, C. E., Bohren, K. M., Lai, C.-J., and Gabbay, K. H. (1995) Human aldose reductase: rate constants for a mechanism including interconversion of ternary complexes by recombinant wild-type enzyme, *Biochemistry 34*, 14323−14330.
44. Wilson, D. K., Nakano, T., Petrash, J. M., Gabbay, K. H., and Quiocho, F. A. (1992) An unlikely sugar substrate site in the 1.65 A structure of the human aldose reductase holoenzyme implicated in diabetic complications, *Science 257*, 81−84.

BI0489762